NIH Public Access
Author Manuscript
J Bone Miner Res. Author manuscript; available in PMC 2015 May 01.

Published in final edited form as:
J Bone Miner Res. 2014 May ; 29(5): 1217–1231. doi:10.1002/jbmr.2114.

Deficiency of Sef is associated with increased postnatal cortical bone mass by regulating Runx2 activity

Qing He, B.S.[1,2], **Xuehui Yang, Ph.D.**[1], **Yan Gong, B.S.**[1,2], **Dmitry Kovalenko, Ph.D.**[1], **Ernesto Canalis, M.D.**[3], **Clifford J. Rosen, M.D.**[1], and **Robert E. Friesel, Ph.D.**[1,2,*]

[1]Center for Molecular Medicine, Maine Medical Center Research Institute Scarborough, ME 04074

[2]Graduate School of Biomedical Sciences and Engineering, University of Maine, Orono, ME

[3]Department of Research, Saint Francis Hospital and Medical Center, Hartford, CT 06105

Abstract

Sef (similar expression to fgf genes) is a feedback inhibitor of fibroblast growth factor (FGF) signaling and functions in part by binding to FGF receptors and inhibiting their activation. Genetic studies in mice and humans indicate an important role for fibroblast growth factor signaling in bone growth and homeostasis. We therefore investigated whether Sef had a function role in skeletal acquisition and remodeling. Sef expression is increased during osteoblast differentiation in vitro, and LacZ staining of *Sef*+/− mice showed high expression of Sef in the periosteum and chondro-osseous junction of neonatal and adult mice. Mice with a global deletion of *Sef* showed increased cortical bone thickness, bone volume and increased periosteal perimeter by μCT. Histomorphometric analysis of cortical bone revealed a significant increase in osteoblast number. Interestingly, *Sef*−/− mice showed very little difference intrabecular bone by μCT and histomorphometry compared to wild type mice. Bone marrow cells from *Sef*−/− mice grown in osteogenic medium showed increased proliferation and increased osteoblast differentiation compared to wild type bone marrow cells. Bone marrow cells from *Sef*−/− mice showed enhanced FGF2-induced activation of the ERK pathway, whereas bone marrow cells from Sef transgenic mice showed decreased FGF2-induced signaling. FGF2-induced acetylation and stability of Runx2 was enhanced in *Sef* −/− bone marrow cells, whereas overexpression of Sef inhibited Runx2-responsive luciferase reporter activity. Bone marrow from *Sef*−/− mice showed enhanced hematopoietic lineage-dependent and osteoblast-dependent osteoclastogenesis and increased bone resorptive activity relative to wild type controls in in vitro assays, while overexpression of Sef inhibited osteoclast differentiation. Taken together, these studies indicate that Sef has specific roles in osteoblast and osteoclast lineages, and that its absence results in increased osteoblast and osteoclast activity with a net increase in cortical bone mass.

[*]Corresponding Author: Robert E. Friesel, Ph.D., Center for Molecular Medicine, Maine Medical Center Research Institute, 81 Research Drive, Scarborough, ME 04074, Phone: 207-396-8147, friesr@mmc.org.

Disclosures:
All authors state that they have no conflicts of interest

Authors roles: Study design: QH, XY and RF. Study conduct: QH. Data collection: QH, DK and EC. Data analysis: QH, EC, and RF. Data interpretation: QH, EC, CR, and RF. Drafting manuscript: QH and RF. Revising manuscript: QH, EC, CR and RF. QH and RF take responsibility for integrity of data analysis.

NIH-PA Author Manuscript
NIH-PA Author Manuscript
NIH-PA Author Manuscript

NIH-PA Author Manuscript

NIH-PA Author Manuscript

NIH-PA Author Manuscript

Keywords

Sef; fibroblast growth factor; osteoblast; osteoclast; differentiation

Introduction

The fibroblast growth factors (FGFs) and their receptors (FGFRs) play important roles in embryonic skeletal development and postnatal bone growth and homeostasis (1–3). Osteoblast growth and differentiation is controlled in part by FGF signaling, but the mechanisms by which this occurs are incompletely understood. Genetic ablation of the *Fgf2* gene in mice results in decreased bone mass and bone formation *in vivo* (4). Conversely, overexpression of FGF2 in transgenic mice leads to skeletal dwarfism (5). Deletion of *Fgfr3* in mice results in increased endochondral bone formation (6, 7), and tissue specific deletion of *Fgfr1* in osteo-chondro-progenitor cells results delayed osteoblast differentiation (8). Similar studies in which *Fgfr2* was deleted in the mouse osteo-chondro-progenitor lineage resulted in skeletal dwarfism and decreased bone mineral density (9). In humans, mutations in *FGFR1* and *FGFR2* cause craniofacial abnormalities (10, 11), whereas mutations in *FGFR3* are associated with dwarfism (12–14). It is apparent from these studies that there is a critical threshold of FGF signaling for normal skeletal growth, above or below which leads to skeletal abnormities.

Recent studies show that there are several mechanisms by which FGF signaling is attenuated. Members of the Sprouty (Spry) family of proteins are feedback inhibitors of receptor tyrosine kinase (RTK) signaling, including FGF signaling, by inhibiting the Ras-Raf-ERK pathway (15, 16) and Sef (similar expression to fgf genes) which appears to target FGFRs specifically (17–20). Sef was identified as an inhibitor of FGF signaling in zebrafish (17, 20), and was shown to physically associate with FGFR1 and FGFR2 and to inhibit FGF-induced receptor tyrosine phosphorylation, resulting in inhibition of both ERK and Akt signaling (18). Furthermore, Sef does not inhibit ERK activation by epidermal growth factor (EGF) or platelet-derived growth factor (PDGF) in NIH3T3 cells, suggesting its function may be restricted to FGFR signaling (18). Gene targeting studies of *Sef* in the mouse revealed that there are no significant embryonic phenotypic abnormalities, however, one study showed that disruption of *Sef* by a gene trap approach produced defects in auditory brainstem development (21–23).

Because FGF signaling is important to skeletal growth and maintenance, and because Sef is an inhibitor of FGF signaling, we sought to investigate its role in skeletal growth and homeostasis. Here we show that Sef loss-of-function *in vivo* results in postnatal increases in cortical bone mass relative to wild type mice. In vitro, loss-of- function of Sef results increased osteoblast and osteoclast differentiation and increased activation of the ERK pathway in osteoblasts in response to FGF2. These results suggest that regulation of the FGF pathway by Sef contributes to the regulation of the postnatal skeleton by balancing FGF signaling.

NIH-PA Author Manuscript

NIH-PA Author Manuscript

NIH-PA Author Manuscript

Materials and Methods

Mice

The Institutional Animal Care and Use Committee at Maine Medical Center approved all experiments involving the use of mice. Sef transgenic mice were generated by using a CAGCAT-Z vector containing a chicken β-actin gene (CAG) promoter-*loxP*-chloramphenicol acetyltransferase (CAT) gene-*loxP*-LacZ was modified by replacing the CAT gene with the open reading frame of green fluorescent protein (GFP) (24). We replaced the LacZ cassette with a V5/His-tagged open reading frame of mouse Sef to create *CAGGFP-Sef* on an FVB background. Upon Cre-mediated recombination, Sef expression is induced, with concomitant loss of GFP reporter gene expression due to Cre-mediated excision of the floxed GFP cassette. B6.Cg-Tg(CAG-cre/Esr1)5Amc/J (*Cre-ERT)* were obtained from the Jackson Laboratory and have been previously described (25). The *KST223* gene trap line was obtained Bay Genomics and the Mutant Mouse Regional Resource Center at UC-Davis. The KST223 mutant mouse was previously characterized (21, 23). The *KST223* mouse (hereafter referred to as *Sef*−/−) contains an insertion of the GT1TMpfs gene trap vector into the third intron of the *Sef* gene. The mice have been crossed onto the C57BL/6J background for more than seven generations. Mice were genotyped by PCR amplification of tail DNA with a three-primer combination: Int3-F2(5′-GCCAAGCCTTGATATGACAAAC-3′) Int3-R1 (5′-TTATGAGTCATTCTCCAGCCCG-3′) for wild-type band; Int3-F2 and GTR1 (5′-GGTCTTTGAGCACCAGAGGACATC-3′) specific for KST223 insertion band as previously described (21). Wild-type littermates served as controls.

Cell culture and differentiation

Primary calvarial osteoblasts were isolated from newborn calvaria by sequential digestion with 0.1% collagenase A (Sigma-Aldrich). Primary osteoblastic cells from the third to fifth fraction were pooled and used for osteoblast differentiation. Bone marrow cells were isolated and cultured by flushing the femurs and tibias of 2-month-old mice as described previously (26). Adherent cell populations were induced to differentiate to the osteoblast lineage in medium supplemented with 100 μg/ml ascorbic acid (Sigma-Aldrich) and 10 mM β-glycerol phosphate (Sigma-Aldrich) for 21 days. Human mesenchymal stem cells (Lonza) were grown in the MSCGM™ mesenchymal stem cell growth medium (Lonza) at 37°C, in 5% CO_2. Upon reaching confluent, human MSCs were cultured using a StemPro Osteogenesis Differentiation Kit (Invitrogen) for 21 days to induce osteogenic differentiation. Periosteal cells were isolated from the femurs and tibia of 2–3 week-old mice by sequential digestion with Collagenase A, and then cultured for 7 days. For osteoclast differentiation, bone marrow cells were cultured in α-MEM containing 10% fetal bovine serum (FBS) with 30 ng/ml macrophage colony-stimulating factor (M-CSF) (Peprotech) and 100 ng/ml receptor activator of nuclear factor kappa-B ligand (RANKL) (Peprotech) for 7 days and then stained for tartrate-resistant acid phosphatase (TRAP) using kit 387-A (Sigma-Aldrich) according to the manufacturer's instructions. For osteoblast-osteoclast co-culture experiments, calvarial osteoblasts were plated at 10^4/well on 24-well plates. The next day, 5×10^5 bone marrow cells were plated into the same wells in medium

NIH-PA Author Manuscript

NIH-PA Author Manuscript

NIH-PA Author Manuscript

containing 10^{-8} M $1,25(OH)_2D_3$ and 10^{-7} prostaglandin E_2. After 6 days, cells positively stained for TRAP containing more than three nuclei were counted as osteoclasts.

Histology

Femurs from 2-month-old male *Sef*+/+ and *Sef*−/− mice were dissected and fixed with 4% paraformaldehyde (PFA) (Sigma-Aldrich). After decalcifying with 10% EDTA (Sigma-Aldrich) pH 7.4 for 2 weeks, femur samples were embedded in paraffin, sectioned and stained with hematoxylin and eosin.

X-Gal staining

Whole mouse embryos at E10.5 were fixed in 4% PFA for 1 h at 4°C, washed in phosphate-buffered saline (PBS), and stained in X-gal solution at 37°C overnight. The femurs from *Sef* +/− were dissected, cleaned of soft tissue and fixed with 4% PFA for 4h at 4°C, washed twice in PBS, and subsequently incubated in X-gal solution at 37°C overnight. After a 1h post-fixation in 4% PFA, P7 femurs were directly processed for paraffin sections, and 2-month-old femurs were decalcified in 10% EDTA for 2 weeks before processing for paraffin sections.

MicroCT analysis

The femurs from *Sef*+/+, +/− and −/− were dissected, cleaned of soft tissue, fixed, and stored in 70% ethanol at 4°C until analysis. Bones were loaded into 12.3-mm-diameter scanning tubes and imaged using a vivaCT 40 scanner to analyze distal trabecular bone and midshaft cortical bone (Scano Medical AG, Brüttisellen, Switzerland) as previously described (27). Units and terminology conform to established guidelines (28).

Alizarin red and alkaline phosphatase staining

Triplicate cultures of bone marrow cells grown in osteogenic medium for 21 days were washed in PBS and fixed in 4% PFA overnight at 4°C. Cells were stained with 1.2% Alizarin red (Sigma-Aldrich) pH 4.2 for 20 min, or labeled using an alkaline phosphatase kit (Sigma-Aldrich). For quantification of Alizarin red staining, 10% (v/v) acetic acid was added to stained monolayer cells and neutralized with 10% (v/v) ammonium hydroxide followed by colorimetric detection at 405 nm as previously described (29).

Hydroxyapatite resorption assay and von Kossa staining

Bone marrow cells were plated at 4×10^5 cells per well in α-MEM containing 10% FBS with M-CSF and RANKL in Corning Osteo Assay Surface 96-well plates (Corning Life Sciences) for 14 days. The plates were stripped with 10% bleach solution for 5 min to remove cells, rinsed and air-dried for staining. Plates were treated in the dark with 100 μl/well 5% (w/v) silver nitrate solution for 30 min. Wells were aspirated and washed, followed by incubation with 100 μl/well 5% (w/v) sodium carbonate (Sigma-Aldrich) in 10% formalin for 4 min at RT. Images were processed using ImageJ software to analyze area of resorption.

NIH-PA Author Manuscript

NIH-PA Author Manuscript

NIH-PA Author Manuscript

cDNA synthesis and quantitative real-time PCR

Total RNA was prepared using the RNeasy Plus Mini Kit (QIAGEN). One microgram of total RNA was used to synthesize first-strand cDNA using the cloned AMV First-stand synthesis kit (New England Biolabs). qRT-PCR analyses of gene expression were performed in triplicate using specific primers and SYBR Green PCR Master Mix (SABioscience). Relative expression levels of the genes of interest were normalized to the housekeeping genes β-actin, cyclophilin (for osteoblast markers) and 36B4 (for osteoclast markers). Data are expressed as fold change over the control at the corresponding time points.

Flow cytometric analysis

Bone marrow cells from *Sef* +/+ and −/−, or from *Sef;Cre-ERT* bitransgenic mice and control littermates either freshly isolated or cultured in α-MEM supplemented with 10% FBS for 1-week were used to analyze subpopulations of mesenchymal progenitor cells. Bone marrow cells labeled by anti-CD45-FITC (eBioscience), anti-CD29-PE (eBioscience) and anti-Sca1-APC (eBioscience) were subjected to FACSCalibur flow cytometer (Becton Dickinson) and analyzed by FlowJo 7.6 software (Treestar). CD29+Sca1+CD45− cells were gated as mesenchymal progenitor cells. Bone marrow cells from *Sef;Cre-ERT* bitransgenic mice were cultured in osteogenic medium with 1μg/ml tamoxifen (Sigma-Aldrich). The cells were incubated with 10μM EdU (5-ethynyl-2′-deoxyuridine) (Invitrogen) for 24 h to measure proliferating cells. Cells that incorporated EdU were labeled with AlexaFluor 488 using the Click-iT EdU Flow Cytometry Assay kit according to the manufacturer's instructions (Invitrogen) and determined by flow cytometric analysis. To quantify apoptotic cells, bone marrow cells cultured in osteogenic medium were double stained with FITC-conjugated annexin V (Invitrogen) and propidium iodide (Sigma-Aldrich) for 15 min in a Ca^{2+}-enriched binding buffer (BD Pharmingen) and then analyzed by FACS.

Colony forming efficiency (CFU-F) of bone marrow stromal cells

Bone marrow cells from *Sef*+/+ and −/− mice, or *Sef;Cre-ERT* bitransgenic mice and control littermates were used to assess colony forming efficiency (CFU-F). The cell suspensions were filtered through 16- and 20-gauge needles to break down cell aggregates. The red blood cells were lysed using EasySep RBC Lysis Buffer (STEMCELL). Nucleated cells were plated in 6-well plate at 1×10^5 cells/well in αMEM + 10% FBS. After 14 days of cultures, the cells were fixed and colonies containing 50 or more cells were counted and CFU (number of colonies per 1×10^5 nucleated marrow cells) was calculated.

Immunoprecipitation and immunoblotting analysis

Bone marrow cells isolated from *Sef* +/+, +/− and −/−, or *CAGGFP-Sef;Cre-ERT* bitransgenic mice and control littermates were cultured until confluent, starved in DMEM, 0.5% FBS overnight and then stimulated with FGF2 (Peprotech) for 10 min. The cells were lysed and subjected to immunoblotting as previous described (30). Immunoblot were probed with antibodies to pRaf (Cell Signaling), pMEK (Cell Signaling) and dpERK (Sigma) as well as total Raf (Cell Signaling), MEK (Cell Signaling) and ERK (Santa Cruz). For immunoprecipitation, bone marrow cells from *Sef* +/+, +/− and −/− mice were serum starved and stimulated with FGF2 for 8 h. Cell lysates were either subjected directly to

NIH-PA Author Manuscript

NIH-PA Author Manuscript

NIH-PA Author Manuscript

immunoblot analysis for Runx2 (Santa Cruz) or incubated with anti-acetyl-lysine (Cell Signaling) overnight for immunoprecipitation. Immune complexes were captured on protein A/G-agarose (Santa Cruz), eluted with 2×SDS sample buffer and immunoblotting performed as previous described (31). Cell lysates prepared from 293T cells that were transiently transfected with Runx2-FLAG and Sef plasmids and the next day treated with inhibitors U0126 (Cell Signaling) (10μM) or HDAC inhibitor Trichostatin A (TSA) (Sigma-Aldrich) (50ng/ml - 1μg/ml) for 24 h. Lysates were immunoprecipitated with anti-FLAG antibody (Sigma) and immunoblotting using anti-acetyl-lysine or anti-Runx2 antibody. Sef antibodies were from R&D Systems.

Luciferase reporter assays

293T cells were co-transfected with 100 ng of osteoblast-specific response element reporter (6OSE-luc) (32) and 3 ng of pRL-SV40, with or without 150 ng Runx2 and 150 ng Sef plasmids in 12-well plates using Genejuice transfection reagent (Novagen). Cells were allowed to recover for 24 hours after transfection, and then incubated with FGF2, U0126 or TSA for another 24 hours. The pRL-SV40 plasmid with a cDNA encoding Renilla luciferase was used as an internal control in each experiment. Activities of firefly and Renilla luciferases were determined sequentially from a single sample with the Dual-luciferase Reporter Assay system (Promega).

Bone histomorphometric analysis

Groups of *Sef* +/+ and −/−, male and female were dual labeled for bone histomorphometric analyses. Mice were injected with 20mg/kg of calcein (Sigma-Aldrich) at 2 months of age and 50mg/kg of demeclocycline (Sigma-Aldrich) 5 days later. Mice were sacrificed 48 h following the demeclocycline injection. Femurs were sectioned on a microtome at a thickness of 5 μm (Microm, Richards-Allan Scientific) and stained with 0.1 % toluidine blue. Static parameters of bone formation and resorption were measured in a defined area between 360 μm and 2160 μm from the growth plate, using an OsteoMeasure morphometry system (Osteometrics) (33). For dynamic histomorphometry, mineralizing surface per bone surface and mineral apposition rate were measured on unstained sections under ultraviolet light, using a triple diamino-2-phenylindole fluorescein set long pass filter, and bone formation rate was calculated. For cortical histomorphometry, femurs were embedded in methyl methacrylate, and cut through the mid diaphysis with an Exakt Precision Saw by Alizee Pathology (Baltimore, MD) and slides were ground using an Exakt 400 CS Micro Grinding System to a thickness of approximately 15 microns and surface polished. Slides were left unstained for fluorescence microscopy or stained with hematoxylin/eosin to establish cellular parameters and analyzed at a magnification of 40x using the OsteoMeasureXP software from OsteoMetrics (Decatur, GA). Stained sections were used to draw the cortical bone, marrow space, osteoid, and cell surfaces as well as to count osteocytes within the cortex, and osteoblasts and osteoclasts along the endocortical surface. The corresponding unstained sections were used to establish mineral apposition rate. The terminology and units used are those recommended by the Histomorphometry Nomenclature Committee of the American Society for Bone and Mineral Research (ASBMR) (34).

NIH-PA Author Manuscript

NIH-PA Author Manuscript

NIH-PA Author Manuscript

Statistical analysis

The unpaired two-tailed Student's *t* test was used to determine the significance of differences between means. *p* values (*$p<0.05$, **$p<0.01$) were considered to be significant.

Results

Sef expression is upregulated during osteogenic differentiation

Because we previously showed that the FGF pathway feedback inhibitors Spry1 and Spry2 are induced during osteoblast differentiation (35), and because FGF2 plays stage specific roles in osteoblast differentiation (2), we investigated whether Sef was expressed during osteoblast differentiation. Calvarial cells from wild-type newborn (P3-5) mice cultured in osteogenic differentiation medium showed an increase in Sef expression during osteoblast differentiation in parallel with increases in markers of osteoblast differentiation (Fig. 1A). A similar pattern of Sef expression was observed in primary bone marrow cells cultured in osteogenic medium (Fig. 1B). We also examined the expression of Sef in human mesenchymal stem cells (hMSC) induced to differentiate to the osteoblast lineage. Sef expression increased in parallel with the osteocalcin (OCN) and alkaline phosphatase (ALP) in hMSC induced to differentiate to osteoblasts (Fig. 1C). Immunoblot analysis of extracts from hMSCs confirmed hSef protein levels increased in a manner consistent with the increase in mRNA during osteoblastic differentiation (Fig. 1D).

Sef deficient mice exhibit increased cortical bone formation

To investigate the role of Sef in postnatal skeletal growth, we used the *Sef* mutant mouse line, *KST223* (21, 23), which was generated during the course of a large-scale gene trap mutagenesis screen and has been used as a *Sef* null mouse model (21). RT-PCR of wild type (*Sef*+/+), heterozygous (*Sef*+/−), and homozygous (*Sef*−/−) embryos showed that there were no detectable wild-type *Sef* transcripts in *Sef*−/− embryos as previously reported (Fig. 2A) (21). X-gal staining of E10.5 *Sef*+/− embryos showed expression of a truncated Sef-β-geo fusion protein in regions of known FGF signaling (Fig. 2B) and is consistent with previous reports (21, 23).

Because Sef is expressed during osteoblast differentiation, and its deletion produces no embryonic skeletal phenotype; we sought to determine whether *Sef* −/− mice had a postnatal skeletal phenotype. MicroCT analysis of the femurs from 2-month-old male *Sef*−/− mice showed significantly increased relative bone volume (BV/TV) (Fig. 2C), reduced cortical bone surface to volume ratio (BS/BV) (Fig. 2D) and increased cortical bone thickness (Fig. 2E and F) compared to controls. Similar changes were observed in female *Sef*−/− mice (Suppl. Fig. 1). Histological analysis of femurs from 2 month-old homozygous *Sef*−/− mice also displayed increased cortical bone thickness (Fig. 2G). However, there was no significant difference between the wild type and *Sef*−/− groups in trabecular bone (Suppl. Table 1). X-gal staining of P7 (Fig. 2H) and 2-month-old (Fig. 2I, J) *Sef*+/− femurs showed that Sef is highly expressed in the periosteum and the chondro-osseous junction of the epiphyseal plate, both regions are rich in osteoprogenitor cells. The osteoprogenitor pools in the periosteum give rise to osteoblasts of the surface of cortical bone. MicroCT analysis showed there was a significant difference in periosteal perimeter between male (Fig. 2K)

NIH-PA Author Manuscript

NIH-PA Author Manuscript

NIH-PA Author Manuscript

and female (Fig. 2L) *Sef*+/+ and *Sef*−/− mice, but no difference in the endosteal perimeter between the two groups (data not shown).

Histomorphometric analysis of cortical bone revealed that there were significant increases in N.Ob/Ec.Pm and N.Ob in *Sef*−/− mice compared with *Sef*+/+ mice, indicating *Sef*−/− mice have significantly increased number of osteoblasts in the cortical bone region (Table 1). The number of osteoblasts in the periosteal layer was not quantified due to technical difficulties associated with identifying osteoblasts in this region. Histomorphometric analysis of trabecular bone showed there were no statistically significant differences between wild type and *Sef*−/− male mice (Table 2). However, in female *Sef*−/− samples, there was a statistically significant increase in osteoclasts and a decrease in trabecular number and an increase in trabecular spacing (Table 2), consistent with the structural changes seen by μCT.

Sef negatively regulate osteogenesis *in vitro*

To investigate whether increased cortical bone thickness in homozygous *Sef*−/− mice was the result of increased osteoblast differentiation, bone marrow cells from wild type and homozygous *Sef*−/− mice were induced to differentiate with osteogenic medium. Bone marrow cells were chosen because previous data showed that Sef expression increased when bone marrow cells were induced to differentiate to the osteoblast lineage. Alkaline phosphatase and Alizarin red staining of *Sef* −/− bone marrow cells showed increased osteogenic differentiation compared to wild type controls (Fig. 3A–C). Quantitative RT-PCR analyses revealed that osteogenic differentiation marker genes were also significantly increased in *Sef*−/− cells (Fig. 3D–F). There was also a small but not statistically significant increase in Runx2 mRNA expression in homozygous *Sef*−/− relative to wild type mice (Fig. 3G).

Because *Sef*−/− mice exhibit increased cortical bone thickness and *Sef* is highly expressed in the periosteum, we also isolated primary periosteal cells from the femurs of and tibia of Sef−/− and wild type mice and cultured them in osteogenic medium for 7 days. Quantitative RT-PCR analyses showed a significant increase in osteoblast marker genes in *Sef*−/− periosteal cells compare to wild type (Fig. 3H). Real-time RT-PCR analyses also revealed increased osteoblast maker gene expression in samples from distal femur metaphysis of *Sef* −/− mice (Fig. 3I).

To test the effects of overexpression of Sef on osteoblast differentiation, we generated transgenic mice with a conditional mouse Sef (mSef) transgene, which efficiently undergoes Cre-mediated recombination to enable inducible expression of Sef (Fig. 4A–C). We crossed female *CAGGFP-Sef* transgenic mice with male *Cre-ERT* transgenic mice, and the resulting bitransgenic offspring (*CAGGFP-Sef;Cre-ERT*) overexpress Sef upon tamoxifen-mediated induction. Tamoxifen-induced over-expression of Sef in cultured bone marrow cells from bitransgenic mice was demonstrated by RT-PCR (Fig. 4B), and by immunoblotting with anti-V5 antibodies to detect the Sef transgenic protein (Fig. 4C). Littermates carrying the Sef transgene, but lacking the tamoxifen-Cre transgene served as controls in these studies.

Bone marrow cells from Sef transgenic mice and control littermates were induced with tamoxifen and cultured in osteogenic medium for 21 days and then stained for alkaline

NIH-PA Author Manuscript

NIH-PA Author Manuscript

NIH-PA Author Manuscript

phosphatase and Alizarin red. Sef over-expression resulted in decreased alkaline phosphatase and Alizarin red staining (Fig. 4D–F), and decreased expression of Opn, Alp and Ocn during osteogenic differentiation, relative to controls (Fig. 4G–I). Sef overexpression also inhibited Runx2 expression to a small extent at later time points (Fig. 4J).

Sef inhibits osteoblast progenitor expansion through decreasing progenitor cell proliferation and inducing apoptosis by inhibiting FGFR/MAPK signaling

Because X-gal staining of adult femurs shows Sef expression in regions rich in osteoprogenitor cells, we investigated whether *Sef*−/− mice had differences in the osteoprogenitor cell population. Fluorescence activated cell sorting (FACS) was performed on whole bone marrow cells that had been triple labeled with anti-CD45-FITC, anti-CD29-PE and anti-Sca1-APC. There was little difference in the number of Sca1+CD29+CD45− cells obtained from freshly isolated bone marrow from *Sef*−/− or wild type mice. However, when bone marrow from *Sef*−/− mice or wild type mice was cultured *in vitro* for one week, the osteoprogenitor population (Sca1+CD29+CD45−) from *Sef*−/− mice was significantly expanded compared to wild type controls (Fig. 5A, Suppl. Fig. 2A, B). Conversely, bone marrow cells from *CAGGFP-Sef;Cre-ERT* mice that overexpress Sef after tamoxifen treatment exhibited fewer osteoprogenitors after one week when compared with wild type controls (Fig. 5B, Suppl. Fig. 2C). In addition, CFU-F assays showed that bone marrow cells from adult *Sef*−/− mice had significantly increased CFU-F expansion compared to wild type cells (Fig. 5C), while overexpression of Sef resulted in reduced colony formation in CFU-F assays (Fig. 5D).

To determine the effect of Sef on proliferation during osteogenic differentiation, bone marrow cells cultured in osteogenic medium were labeled with EdU for 24 hours and analyzed by flow cytometry. Bone marrow cells from *Sef*−/− mice showed a small but significant increase in EdU+ cells compared to wild type controls (Fig. 5E, Suppl. Fig. 2D). In contrast, bone marrow cells from *CAGGFP-Sef;Cre-ERT* mice induced to express Sef with tamoxifen, showed significantly reduced EdU incorporation compared to controls (Fig. 5F, Suppl. Fig. 2E). We also performed annexin V/propidium iodide double labeling and flow cytometric analyses to detect apoptotic cells in differentiating bone marrow cells. FACS results revealed lower rates of apoptosis in differentiating bone marrow cells from *Sef* −/− mice compared to wild type controls, whereas over-expression of *Sef* significantly increased the number of apoptotic cells (Fig. 5G, H, Suppl. Fig. 2F, G).

To explore the role of Sef in FGF-induced ERK activation during osteoblastogenesis, bone marrow cells from *CAGGFP-Sef;Cre-ERT* were induced to express Sef using tamoxifen, and cultured until confluent. After serum starvation, the cells were stimulated with FGF2 for 10 min. Over-expression of Sef resulted in a reduction of FGF2-induced pRaf, pMEK, and dpERK compared to control cultures. Overall levels of Raf, MEK and ERK1/2 were unaffected (Fig. 5I). Similar experiments were performed using bone marrow cells from *Sef* −/−, and +/+ mice. *Sef* −/− cells showed enhanced FGF2-induced, pRaf, pMEK and dpERK (Fig. 5J). In addition, pRaf was increased in *Sef*−/− bone marrow cells in the absence of FGF2.

NIH-PA Author Manuscript

NIH-PA Author Manuscript

NIH-PA Author Manuscript

Sef represses osteogenic differentiation in part by decreasing FGF/MAPK signaling, Runx2 acetylation, and transcriptional activity

FGF2 has been shown to activate the Runx2 transcription factor in osteoblasts through post-translational modifications (36), and FGF2 increases Runx2 protein stability and acetylation levels in part through an ERK-dependent mechanism (37, 38). To address the role of Sef on Runx2 acetylation, bone marrow cells from *Sef*+/+, *Sef*+/− and *Sef*−/− mice were stimulated with or without FGF2 after serum starvation. Acetylated and total Runx2 protein levels were increased upon FGF2 stimulation in *Sef*−/− bone marrow cells, and also showed an increase in total Runx2 and acetylated Runx2 even without FGF2 stimulation compare to *Sef*+/+ control cells (Fig. 6A). Immunohistochemical staining of P0 femurs from *Sef*+/+ and *Sef*−/− showed increased Runx2 in the periosteal layer of *Sef*−/− mice (Suppl. 3A, B).

We wondered whether Sef overexpression would inhibit Runx2 acetylation and transcriptional activity. 293T cells were co-transfected with the 6OSE-Luciferase Runx2 reporter construct, and a FLAG-tagged Runx2 expression plasmid either with or without a Sef expression vector. Twenty-four hours after transfection, the cells were treated with the MEK inhibitor U0126 or the HDAC inhibitor TSA. Over-expression of Sef, as well as treatment with U0126 significantly reduced Runx2-induced luciferase reporter activity (Fig. 6B). Moreover, Sef-mediated repression of Runx2 transcriptional activity could be reversed by TSA in a dose-dependent manner. Immunoblot analysis shows that acetylated Runx2 levels were decreased by overexpression of Sef or by U0126 treatment, and these reductions were rescued by TSA treatment (Fig. 6C). We also show that overexpression of Sef or treatment with U0126 dramatically reduced FGF2-induced OSE reporter activity (Fig. 6D).

Sef impairs multinucleated osteoclast differentiation and function

Analysis of bone marrow cells from *Sef*+/+ and *Sef*−/− mice grown in M-CSF and RANKL-containing osteoclastogenic medium showed significantly more TRAP-positive osteoclasts in *Sef*−/− cultures than in *Sef*+/+ cultures, and the increased osteoclast formation by knocking out Sef could be fully rescued by U0126 treatment (Fig. 7A, B). Bone marrow cells from *CAGGFP-Sef;Cre-ERT* mice treated with tamoxifen produced fewer osteoclasts than cells from Cre-negative littermates control cultures (Fig. 7C, D). U0126-treated cultures had fewer osteoclasts when compared with DMSO-treated bone marrow cells (Suppl. Fig. 4A, B).

The expression of osteoclast differentiation marker genes was examined by qRT-PCR. The mRNA expression level of osteoclast marker genes *Tracp*, *Nfatc1*, and *Ctsk* were markedly elevated in osteoclast cultures from *Sef*−/− mice relative to *Sef*+/+ mice (Fig. 7E–G). In contrast, bone marrow cells from *CAGGFP-Sef;Cre-ERT* transgenic mice induced to express Sef showed significantly decreased expression of *Tracp*, *Nfatc1* and *Ctsk* (Fig. 7H–J) compared with single transgenic littermates which did not over-express Sef.

Osteoclast differentiation in an ex vivo co-culture system with calvarial osteoblasts and bone marrow cells showed that when either osteoblasts or bone marrow cells were derived from *Sef*−/− mice osteoclastogenesis was enhanced, and this effect was further enhanced when both osteoblasts and bone marrow were from *Sef*−/− mice (Fig. 8A, B). This indicates that

NIH-PA Author Manuscript

NIH-PA Author Manuscript

NIH-PA Author Manuscript

Sef acts as a negative regulator for osteoclast precursors in a cell autonomous manner and for osteoblasts to support osteoclast differentiation. The main mechanism by which osteoblasts regulate osteoclastogenesis involves the secretion of RANKL and OPG. We therefore measured the RANKL and OPG mRNA expression levels as well as RANKL/OPG ratio in co-cultured calvarial osteoblasts and bone marrow cells. *Sef*−/− calvarial osteoblasts and *Sef*−/− bone marrow cell co-cultures expressed significantly more RANKL than control cells, while OPG expression was unaffected. Thus, deletion of *Sef* increases the RANKL/OPG ratio, enhancing osteoclastogenesis (Fig. 8C). RNA samples from the distal femur metaphysis of *Sef*−/− mice also exhibited significantly increased RANKL mRNA level and RANKL/OPG ratio when compared with wild type (Fig. 8D), suggesting Sef regulates osteoblast-dependent osteoclastogenesis.

To determine whether Sef regulates osteoclast resorptive activity we performed hydroxyapatite resorption assays with bone marrow cell-derived osteoclasts from *Sef*+/+ and *Sef*−/− mice. *Sef*−/− osteoclasts showed a significant increase in the resorption area compared with wild-type controls, and the increased osteoclast resorptive activity could be reversed by adding U0126 (Fig. 9A, B). Similar experiments were performed using bone marrow cells from *CAGGFP-Sef;Cre-ERT* transgenic mice induced to express Sef. Data show that overexpression of Sef resulted in decreased osteoclast resorption area and activity (Fig. 9C, D).

Discussion

Sef was originally identified as a feedback inhibitor of FGF signaling in zebrafish and in cell culture models (17, 18, 20, 39). Other studies suggest that Sef may inhibit ERK activation and localization directly (40). Previous studies have shown that components of the ERK pathway are important to osteoblast differentiation and bone formation. It was reported that targeted deletion of ERK1 and ERK2 in osteoprogenitor cells inhibited osteoblast differentiation and in the absence of ERK1 and ERK2 mature *Ocn*-expressing osteoblasts do not develop suggesting that ERK1/2 are necessary for osteoblast maturation (41). Furthermore, *Prx1-MEK1* transgenic mice that express a constitutively active MEK1 mutant in the periosteum/perichondrium show increased postnatal cortical bone thickness (41). Our data show that expression of Sef in osteoblast progenitors dampens ERK signaling, osteoblast expansion and differentiation whereas deletion of Sef in osteoblasts enhances ERK activation, proliferation and differentiation. Furthermore, we show that LacZ expression in *Sef* +/− mice is highest in the periosteum of postnatal and adult mice, the same regions most sensitive to ERK ablation. Thus our data are consistent with the notion that loss of Sef results in increased ERK signaling, increased expansion of osteoprogenitor cells and increased osteoblast differentiation, resulting in increased cortical bone thickness similar to *Prx1-MEK1* transgenic mice.

Runx2 is a transcription factor that is essential for osteoblast differentiation and regulates the expression of osteoblast marker genes such as osteocalcin, osteopontin and alkaline phosphatase (37). FGF2 signaling induces Runx2 expression in part through a protein kinase C (PKC)-dependent mechanism, and FGF signaling induces ERK-mediated phosphorylation of Runx2 protein, which increases its transcriptional activity (38). Recently, it was shown

NIH-PA Author Manuscript

NIH-PA Author Manuscript

NIH-PA Author Manuscript

that FGF2-mediated ERK signaling increases Runx2 acetylation and stabilization also leading to increased transcriptional activity (32). Our data show that loss of Sef has negligible effects on Runx2 mRNA expression, however osteoprogenitor cells from *Sef*−/− mice showed enhanced Runx2 acetylation, and this was further increased by treatment with FGF2. Conversely, overexpression of Sef decreased Runx2 expression at late stages of osteoblast differentiation, and decreases Runx2 acetylation and transcriptional activity. These data are in agreement with the report that Runx2 expression occurs normally in ERK1/2 deficient osteoprogenitors but expression of mature osteoblast genes such as *Ocn* are impaired. Because endogenous Sef expression increases during osteoblast differentiation of osteoprogenitors in vitro, together with our gain- and loss-of-function data, this suggests that Sef may act to attenuate FGF signaling at later stages of osteoblast differentiation. Thus, our data suggest that Sef may act to modulate FGF-mediated ERK signaling and Runx2 stability and transcriptional activity. Our current data do not exclude the possibility that Sef may affect other pathways that regulate ERK activation in osteoblasts such as BMP2 or TGF-β1 (42). However, our previous studies indicate that Sef inhibits FGF2 but not PDGF or EGF induced ERK activation in NIH 3T3 cells, and thus the observed effects are likely to be FGF specific. This may in part explain why the limb phenotype in *Sef*−/− mice is less severe than that reported for *MEK1;Prx1-Cre* mice which likely activates ERK to a greater extent in osteoprogenitors than derepression of ERK activation by FGF2 signaling though loss of Sef. If loss of Sef were to lead to derepression of other pathways that lead to ERK activation, it would be anticipated that the *Sef*−/− phenotype would be more similar to *MEK1;Prx1-Cre* mice.

Because the *Sef*−/− mouse model that we used in these studies was a gene trap, we cannot exclude the possibility that loss of Sef affects cell types other than osteoblasts to produce the skeletal phenotype. Indeed our studies show that loss of Sef function results in increased osteoclast differentiation and bone resorption activity. It was recently reported that ERK1 positively regulates osteoclast differentiation and function (43), and therefore *Sef* deficiency in osteoclasts may enhance ERK activity as it does in osteoblasts resulting in greater differentiation and function of osteoclasts in *Sef* deficient mice. This conclusion is further supported by our observation that transgenic expression of Sef in bone marrow cultures results in diminished osteoclast differentiation and function. Furthermore, use of the ERK inhibitor U0126 completely reversed the increase in osteoclast differentiation bone resorption activity as a result of Sef deletion. Thus, Sef plays a role of osteoclast function, in part by regulating ERK activation. Because the *Sef*−/− mouse model that we used in these studies was a gene trap, further study will be required using tissue specific gene targeting strategies to determine more specifically mechanisms by which Sef regulates osteoclast and osteoblast function.

Adult bone mass is determined by the balance of bone formation by osteoblasts and bone resorption by osteoclasts. We found that global deletion of Sef affects the balance of bone remodeling by affecting both osteoblastogenesis and osteoclastogenesis. Sef functions as a coordinator for bone homeostasis that balances the activities of osteoblasts and osteoclasts to regulate bone mass.

NIH-PA Author Manuscript

NIH-PA Author Manuscript

NIH-PA Author Manuscript

Histomorphometric and μCT data show that trabecular bone was relatively unaffected in *Sef* −/− mice, however there was a statistically significant increase in cortical bone thickness, bone volume, and osteoblast number in *Sef*−/− cortical bone. In addition, β-galactosidase staining of *Sef*+/− femurs showed highest levels of expression in the periosteum. Thus, it appears that *in vivo*, Sef may play a greater role in the regulation of periosteal osteoprogenitor growth and differentiation than in the trabecular osteoprogenitor pool. Further study will reveal whether there are unique differences in periosteal and trabecular osteoprogenitors that make them variously sensitive to Sef loss of function.

Our study shows for the first time the role of Sef in bone homeostasis. In summary, Sef regulates cortical bone growth, and that its deletion results in increased FGF2-mediated Runx2 acetylation in osteoblasts and increased osteoblast proliferation and differentiation presumably through an ERK-dependent mechanism (Suppl. Fig. 5). Although osteoclast differentiation and function are also enhanced in Sef−/− mice, our data suggest that the overall balance in bone remodeling favors cortical bone formation. The increase in bone mass in Sef deficient mice is most notable in the cortical bone, a region where Sef is normally highly expressed, suggesting a unique function for Sef in this skeletal compartment. Because members of the Sprouty family of proteins also negatively regulate FGF signaling, and Sprouty's are expressed in skeletal elements, it is possible that loss of Sef is partially compensated for by Sprouty family members resulting in a mild phenotype. Further study on the mechanisms of negative regulation of FGF signaling in skeletal growth and homeostasis will be required to ascertain the relative contributions of Sef and Sprouty to normal skeletal growth and maintenance.

Supplementary Material

Refer to Web version on PubMed Central for supplementary material.

Acknowledgments

We thank Lindsey Gower for expert technical assistance and members of the Rosen lab for helpful discussions. We thank Terry Henderson for μCT analysis, Anne Harrington for assistance in the generation of the Sef transgenic mice, Katrina Abramo and Grazina Mangoba for histology, and Allison Kent for bone histomorphometry. This work was support by NIH grants R01 DK73781 and P30RR030927/P30GM103392 (transgenic mouse and small animal imaging core, histology core) R. Friesel, PI, P20RR181789/P20GM103465 (cell phenotyping and progenitor cell analysis cores) to D.M. Wojchowski, PI, R01 AR021707 to E. Canalis, R24DK092759 to C. Rosen, and institutional support from the Maine Medical Center. Yan Gong was the recipient of a predoctoral fellowship from the Founders Affiliate of the American Heart Association.

References

1. Ornitz DM, Marie PJ. FGF signaling pathways in endochondral and intramembranous bone development and human genetic disease. Genes Dev. 2002 Jun 15; 16(12):1446–65. [PubMed: 12080084]
2. Su N, Du X, Chen L. FGF signaling: its role in bone development and human skeleton diseases. Front Biosci. 2008; 13:2842–65. [PubMed: 17981758]
3. Canalis E. Growth factor control of bone mass. J Cell Biochem. 2009 Nov 1; 108(4):769–77. [PubMed: 19718659]
4. Montero A, Okada Y, Tomita M, Ito M, Tsurukami H, Nakamura T, Doetschman T, Coffin JD, Hurley MM. Disruption of the fibroblast growth factor-2 gene results in decreased bone mass and bone formation. J Clin Invest. 2000 Apr; 105(8):1085–93. [PubMed: 10772653]

NIH-PA Author Manuscript NIH-PA Author Manuscript NIH-PA Author Manuscript

5. Coffin JD, Florkiewicz RZ, Neumann J, Mort-Hopkins T, Dorn GW 2nd, Lightfoot P, German R, Howles PN, Kier A, O'Toole BA, et al. Abnormal bone growth and selective translational regulation in basic fibroblast growth factor (FGF-2) transgenic mice. Mol Biol Cell. 1995 Dec; 6(12):1861–73. Research Support, Non-U.S. Gov't Research Support, U.S. Gov't, P.H.S. [PubMed: 8590811]

6. Colvin JS, Bohne BA, Harding GW, McEwen DG, Ornitz DM. Skeletal overgrowth and deafness in mice lacking fibroblast growth factor receptor 3. Nat Genet. 1996 Apr; 12(4):390–7. [PubMed: 8630492]

7. Deng C, Wynshaw-Boris A, Zhou F, Kuo A, Leder P. Fibroblast growth factor receptor 3 is a negative regulator of bone growth. Cell. 1996 Mar 22; 84(6):911–21. [PubMed: 8601314]

8. Jacob AL, Smith C, Partanen J, Ornitz DM. Fibroblast growth factor receptor 1 signaling in the osteo-chondrogenic cell lineage regulates sequential steps of osteoblast maturation. Dev Biol. 2006 Aug 15; 296(2):315–28. [PubMed: 16815385]

9. Yu K, Xu J, Liu Z, Sosic D, Shao J, Olson EN, Towler DA, Ornitz DM. Conditional inactivation of FGF receptor 2 reveals an essential role for FGF signaling in the regulation of osteoblast function and bone growth. Development. 2003 Jul; 130(13):3063–74. [PubMed: 12756187]

10. Hatch NE. FGF signaling in craniofacial biological control and pathological craniofacial development. Crit Rev Eukaryot Gene Expr. 2010; 20(4):295–311. [PubMed: 21395503]

11. Reardon W, Winter RM, Rutland P, Pulleyn LJ, Jones BM, Malcolm S. Mutations in the fibroblast growth factor receptor 2 gene cause Crouzon syndrome. Nat Genet. 1994 Sep; 8(1):98–103. [PubMed: 7987400]

12. Webster MK, Donoghue DJ. FGFR activation in skeletal disorders: too much of a good thing. Trends Genet. 1997 May; 13(5):178–82. [PubMed: 9154000]

13. Rousseau F, Bonaventure J, Legeai-Mallet L, Pelet A, Rozet JM, Maroteaux P, Le Merrer M, Munnich A. Mutations in the gene encoding fibroblast growth factor receptor-3 in achondroplasia. Nature. 1994 Sep 15; 371(6494):252–4. [PubMed: 8078586]

14. Shiang R, Thompson LM, Zhu YZ, Church DM, Fielder TJ, Bocian M, Winokur ST, Wasmuth JJ. Mutations in the transmembrane domain of FGFR3 cause the most common genetic form of dwarfism, achondroplasia. Cell. 1994 Jul 29; 78(2):335–42. [PubMed: 7913883]

15. Mason JM, Morrison DJ, Basson MA, Licht JD. Sprouty proteins: multifaceted negative-feedback regulators of receptor tyrosine kinase signaling. Trends Cell Biol. 2006 Jan; 16(1):45–54. [PubMed: 16337795]

16. Edwin F, Anderson K, Ying C, Patel TB. Intermolecular interactions of Sprouty proteins and their implications in development and disease. Mol Pharmacol. 2009 Oct; 76(4):679–91. [PubMed: 19570949]

17. Furthauer M, Lin W, Ang SL, Thisse B, Thisse C. Sef is a feedback-induced antagonist of Ras/MAPK-mediated FGF signalling. Nat Cell Biol. 2002 Feb; 4(2):170–4. [PubMed: 11802165]

18. Kovalenko D, Yang X, Nadeau RJ, Harkins LK, Friesel R. Sef inhibits fibroblast growth factor signaling by inhibiting FGFR1 tyrosine phosphorylation and subsequent ERK activation. J Biol Chem. 2003 Apr 18; 278(16):14087–91. [PubMed: 12604616]

19. Tsang M, Dawid IB. Promotion and attenuation of FGF signaling through the Ras-MAPK pathway. Sci STKE. 2004 Apr 13.2004(228):pe17. [PubMed: 15082862]

20. Tsang M, Friesel R, Kudoh T, Dawid IB. Identification of Sef, a novel modulator of FGF signalling. Nat Cell Biol. 2002 Feb; 4(2):165–9. [PubMed: 11802164]

21. Abraira VE, Hyun N, Tucker AF, Coling DE, Brown MC, Lu C, Hoffman GR, Goodrich LV. Changes in Sef levels influence auditory brainstem development and function. J Neurosci. 2007 Apr 18; 27(16):4273–82. [PubMed: 17442811]

22. Lin W, Jing N, Basson MA, Dierich A, Licht J, Ang SL. Synergistic activity of Sef and Sprouty proteins in regulating the expression of Gbx2 in the mid-hindbrain region. Genesis. 2005 Mar; 41(3):110–5. [PubMed: 15729686]

23. Leighton PA, Mitchell KJ, Goodrich LV, Lu X, Pinson K, Scherz P, Skarnes WC, Tessier-Lavigne M. Defining brain wiring patterns and mechanisms through gene trapping in mice. Nature. 2001 Mar 8; 410(6825):174–9. [PubMed: 11242070]

NIH-PA Author Manuscript

NIH-PA Author Manuscript

NIH-PA Author Manuscript

24. Yang X, Harkins LK, Zubanova O, Harrington A, Kovalenko D, Nadeau RJ, Chen PY, Toher JL, Lindner V, Liaw L, Friesel R. Overexpression of Spry1 in chondrocytes causes attenuated FGFR ubiquitination and sustained ERK activation resulting in chondrodysplasia. Dev Biol. 2008 Sep 1; 321(1):64–76. [PubMed: 18582454]
25. Hayashi S, McMahon AP. Efficient recombination in diverse tissues by a tamoxifen-inducible form of Cre: a tool for temporally regulated gene activation/inactivation in the mouse. Dev Biol. 2002 Apr 15; 244(2):305–18. [PubMed: 11944939]
26. Kawai M, Breggia AC, DeMambro VE, Shen X, Canalis E, Bouxsein ML, Beamer WG, Clemmons DR, Rosen CJ. The heparin-binding domain of IGFBP-2 has insulin-like growth factor binding-independent biologic activity in the growing skeleton. J Biol Chem. 2011 Apr 22; 286(16):14670–80. [PubMed: 21372140]
27. Urs S, Venkatesh D, Tang Y, Henderson T, Yang X, Friesel RE, Rosen CJ, Liaw L. Sprouty1 is a critical regulatory switch of mesenchymal stem cell lineage allocation. FASEB J. 2010 Sep; 24(9): 3264–73. [PubMed: 20410440]
28. Bouxsein ML, Boyd SK, Christiansen BA, Guldberg RE, Jepsen KJ, Muller R. Guidelines for assessment of bone microstructure in rodents using micro-computed tomography. Journal of bone and mineral research: the official journal of the American Society for Bone and Mineral Research. 2010 Jul; 25(7):1468–86. Review.
29. Gregory CA, Gunn WG, Peister A, Prockop DJ. An Alizarin red-based assay of mineralization by adherent cells in culture: comparison with cetylpyridinium chloride extraction. Anal Biochem. 2004 Jun 1; 329(1):77–84. Comparative Study Research Support, Non-U.S. Gov't Research Support, U.S. Gov't, P.H.S. [PubMed: 15136169]
30. Chen PY, Simons M, Friesel R. FRS2 via FGFR1 is required for PDGFRbeta -mediated regulation of vascular smooth muscle marker gene expression. J Biol Chem. 2009 Apr 1.
31. Chen PY, Friesel R. FGFR1 forms an FRS2-dependent complex with mTOR to regulate smooth muscle marker gene expression. Biochem Biophys Res Commun. 2009 May 1; 382(2):424–9. [PubMed: 19285959]
32. Park OJ, Kim HJ, Woo KM, Baek JH, Ryoo HM. FGF2-activated ERK mitogen-activated protein kinase enhances Runx2 acetylation and stabilization. The Journal of biological chemistry. 2010 Feb 5; 285(6):3568–74. Research Support, Non-U.S. Gov't. [PubMed: 20007706]
33. Canalis E, Zanotti S, Beamer WG, Economides AN, Smerdel-Ramoya A. Connective tissue growth factor is required for skeletal development and postnatal skeletal homeostasis in male mice. Endocrinology. 2010 Aug; 151(8):3490–501. Research Support, N.I.H., Extramural. [PubMed: 20534727]
34. Parfitt AM, Drezner MK, Glorieux FH, Kanis JA, Malluche H, Meunier PJ, Ott SM, Recker RR. Bone histomorphometry: standardization of nomenclature, symbols, and units. Report of the ASBMR Histomorphometry Nomenclature Committee. Journal of bone and mineral research: the official journal of the American Society for Bone and Mineral Research. 1987 Dec; 2(6):595–610.
35. Yang X, Webster JB, Kovalenko D, Nadeau RJ, Zubanova O, Chen PY, Friesel R. Sprouty genes are expressed in osteoblasts and inhibit fibroblast growth factor-mediated osteoblast responses. Calcif Tissue Int. 2006 Apr; 78(4):233–40. [PubMed: 16604287]
36. Komori T. Signaling networks in RUNX2-dependent bone development. Journal of cellular biochemistry. 2011 Mar; 112(3):750–5. Review. [PubMed: 21328448]
37. Franceschi RT, Xiao G. Regulation of the osteoblast-specific transcription factor, Runx2: Responsiveness to multiple signal transduction pathways. J Cell Biochem. 2003; 88(3):446–54. [PubMed: 12532321]
38. Xiao G, Jiang D, Gopalakrishnan R, Franceschi RT. Fibroblast growth factor 2 induction of the osteocalcin gene requires MAPK activity and phosphorylation of the osteoblast transcription factor, Cbfa1/Runx2. J Biol Chem. 2002 Sep 27; 277(39):36181–7. [PubMed: 12110689]
39. Kovalenko D, Yang X, Chen PY, Nadeau RJ, Zubanova O, Pigeon K, Friesel R. A role for extracellular and transmembrane domains of Sef in Sef-mediated inhibition of FGF signaling. Cell Signal. 2006 Nov; 18(11):1958–66. [PubMed: 16603339]
40. Torii S, Kusakabe M, Yamamoto T, Maekawa M, Nishida E. Sef is a spatial regulator for Ras/MAP kinase signaling. Dev Cell. 2004 Jul; 7(1):33–44. [PubMed: 15239952]

NIH-PA Author Manuscript

NIH-PA Author Manuscript

NIH-PA Author Manuscript

41. Matsushita T, Chan YY, Kawanami A, Balmes G, Landreth GE, Murakami S. Extracellular signal-regulated kinase 1 (ERK1) and ERK2 play essential roles in osteoblast differentiation and in supporting osteoclastogenesis. Molecular and cellular biology. 2009 Nov; 29(21):5843–57. [PubMed: 19737917]

42. Lee KS, Kim HJ, Li QL, Chi XZ, Ueta C, Komori T, Wozney JM, Kim EG, Choi JY, Ryoo HM, Bae SC. Runx2 is a common target of transforming growth factor beta1 and bone morphogenetic protein 2, and cooperation between Runx2 and Smad5 induces osteoblast-specific gene expression in the pluripotent mesenchymal precursor cell line C2C12. Molecular and cellular biology. 2000 Dec; 20(23):8783–92. [PubMed: 11073979]

43. He Y, Staser K, Rhodes SD, Liu Y, Wu X, Park SJ, Yuan J, Yang X, Li X, Jiang L, Chen S, Yang FC. Erk1 positively regulates osteoclast differentiation and bone resorptive activity. PLoS One. 2011; 6(9):e24780. [PubMed: 21961044]

NIH-PA Author Manuscript
NIH-PA Author Manuscript
NIH-PA Author Manuscript

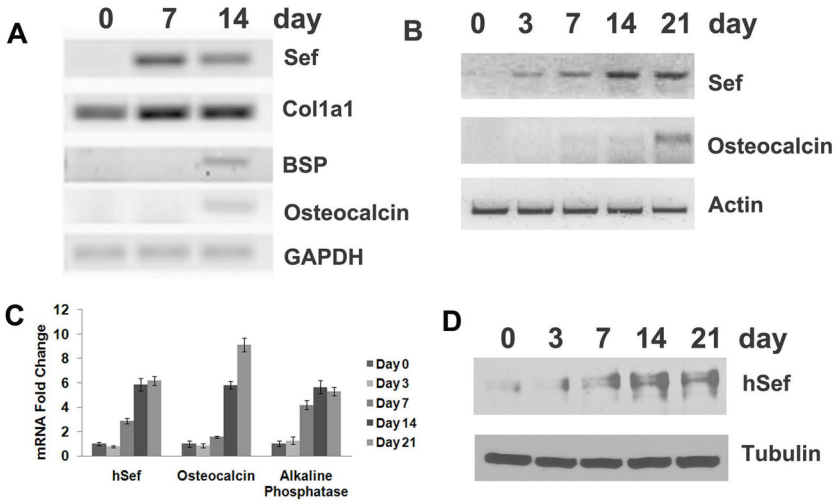

Figure 1. Sef expression is induced during osteogenic differentiation

(A) Primary calvarial osteoblasts from newborn mice and (B) bone marrow cells from adult mice were grown in osteogenic differentiation medium for up to 14 days or 21 days. Expression levels of Sef and osteogenic differentiation genes were determined by RT-PCR. Sef expression was determined in human mesenchymal stem cells grown in osteogenic differentiation medium for 21 days by RT-qPCR (C) and immunoblotting (D).

NIH-PA Author Manuscript
NIH-PA Author Manuscript
NIH-PA Author Manuscript

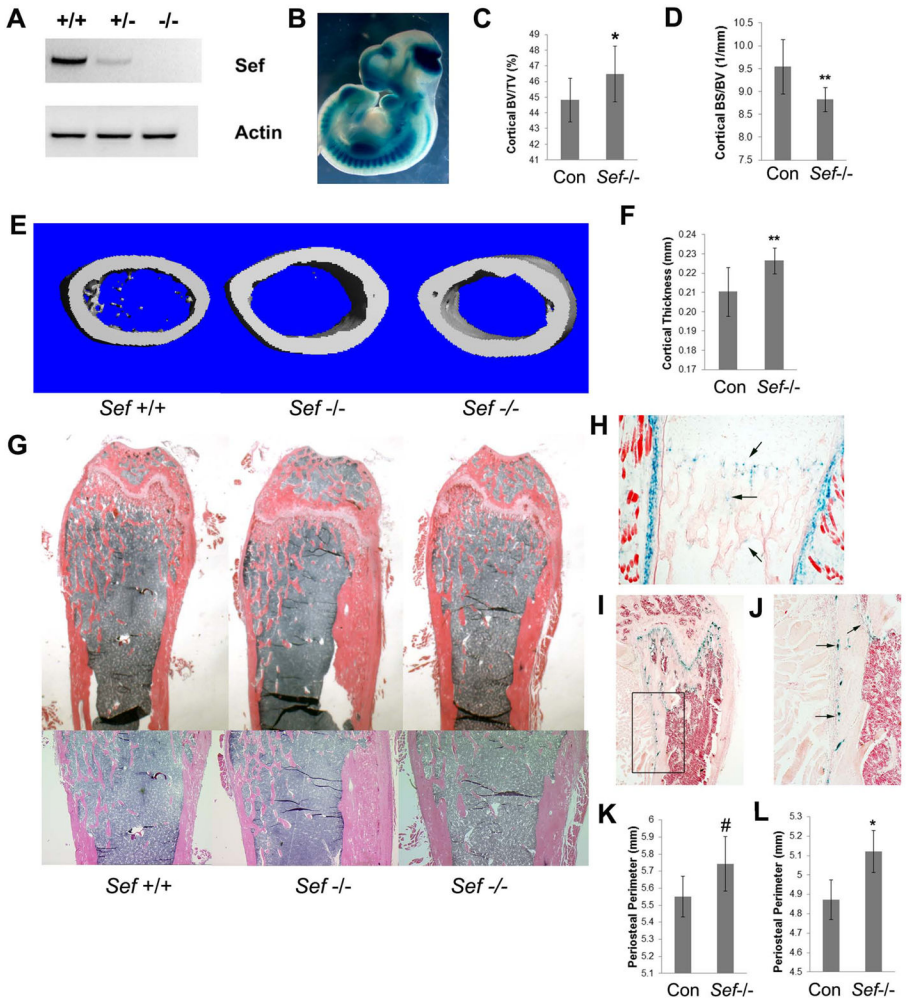

Figure 2. *Sef*−/− mice show increased postnatal cortical bone thickness

(A) Sef mRNA expression in E12.5 *Sef*+/+, +/−, −/− embryos. (B) Whole mount X-gal staining of an E10.5 *Sef*+/− embryo showing expression pattern of Sef. (C–F) μCT analysis of femoral cortical thickness, BV/TV and BS/BV of the control group (2-month-old *Sef*+/+, and *Sef*+/−, n=24) and KO group (2-month-old *Sef*−/−, n=13), shows significant difference between two groups (**p*<0.05; ***p*<0.01). (E) μCT image of the femoral cortical area of 2-month-old *Sef*+/+and *Sef*−/− mice, (G) Hematoxylin and eosin staining of femur samples from 2-month-old *Sef*+/+ and *Sef*−/− mice. (H) X-gal staining of P7 *Sef*+/− femur. (I) X-gal staining of 2-month-old *Sef*+/− femur. (J) Enlarged boxed in area from panel I. (K) Increased periosteal perimeter in male *Sef*−/− mice. (L) Significantly increased periosteal perimeter in female *Sef*−/− mice. #p = 0.084, *p = 0.032 versus *Sef*+/+ wild type controls.

NIH-PA Author Manuscript
NIH-PA Author Manuscript
NIH-PA Author Manuscript

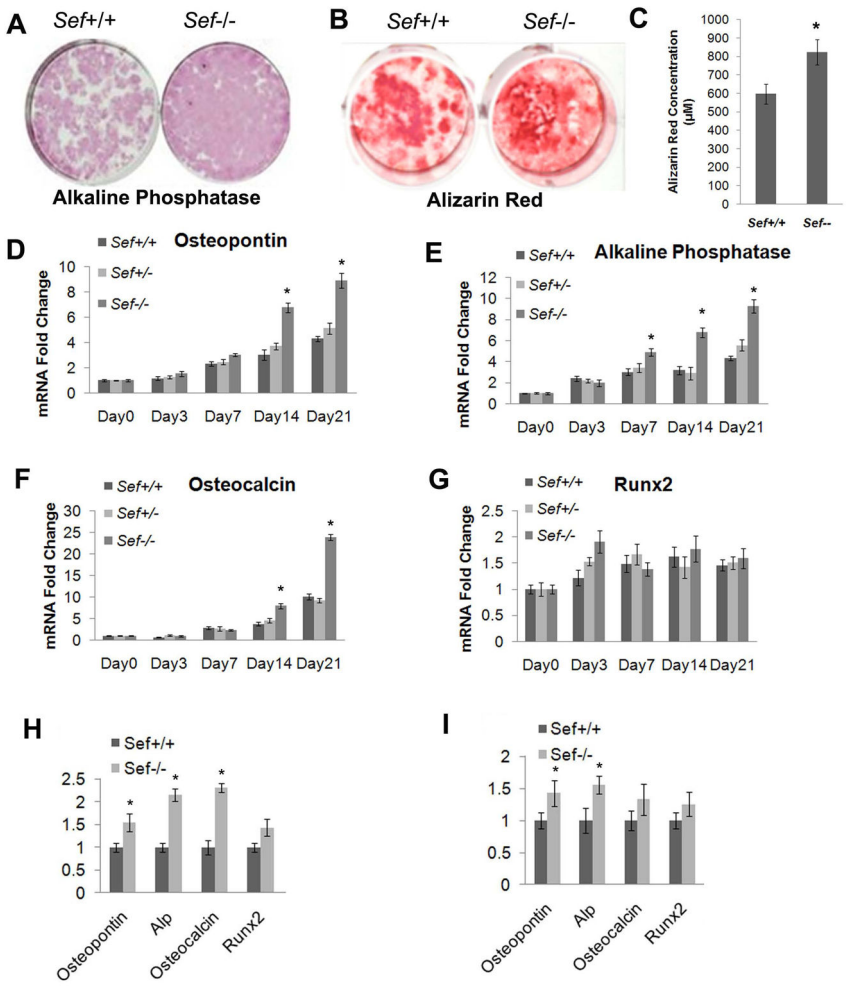

Figure 3. Osteoblast differentiation is enhanced in bone marrow cells from *Sef*−/− mice

Bone marrow cells isolated from *Sef*−/− mice and *Sef*+/+ were cultured in osteogenic differentiation medium for 21 days and stained for (A) alkaline phosphatase and (B) Alizarin red. (C) Alizarin red concentration was quantified spectrophotometrically after extraction of the stain from samples in B (n=3). RT-qPCR analysis showing mRNA expression of osteogenic differentiation markers: (D) osteopontin; (E) alkaline phosphatase; (F) osteocalcin and (G) Runx2 (n=4). (H) RNA was extracted from primary periosteal cells for RT-qPCR analysis for osteogenic differentiation markers (n=3). (I) RNA isolated from distal femur metaphysis were quantified by RT-qPCR for osteogenic differentiation markers (n=3).

NIH-PA Author Manuscript
NIH-PA Author Manuscript
NIH-PA Author Manuscript

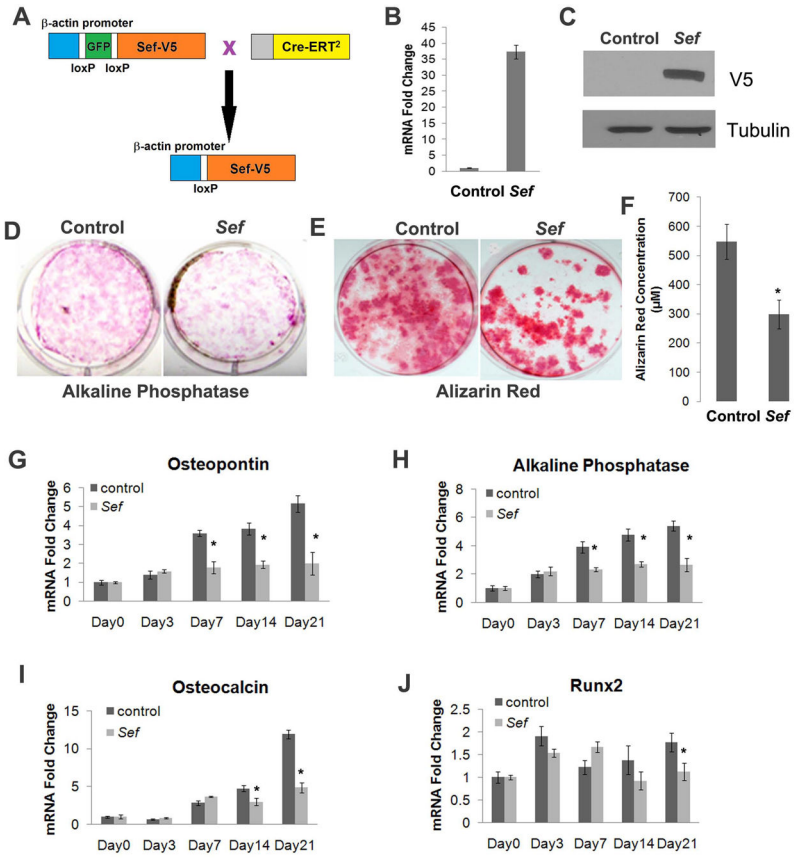

Figure 4. Overexpression of Sef inhibits osteoblastic differentiation

(A) Schematic representation for the tamoxifen Cre-inducible expression of Sef. (B, C) Bone marrow cells were isolated from *Sef;Cre-ERT*^{2} double-transgenic mice and their control (*CAGGFP-Sef*) littermates and cultured with tamoxifen to induce Sef over-expression. Over-expression of Sef was determined by (B) RT-qPCR and (C) immunoblotting. (D, E) Bone marrow cells from *Sef;Cre-ERT*^{2} double-transgenic and control mice were cultured in osteogenic differentiation medium with for 21 days and stained for (D) alkaline phosphatase and (E) Alizarin red. (F) Quantification of Alizarin red concentration between *Sef;Cre-ERT*^{2} double-transgenic mice and their control samples (n=3). RT-qPCR analysis showing mRNA expression of osteogenic differentiation markers: (G) osteopontin; (H) alkaline phosphatase; (I) osteocalcin and (J) Runx2 (n=5).

NIH-PA Author Manuscript
NIH-PA Author Manuscript
NIH-PA Author Manuscript

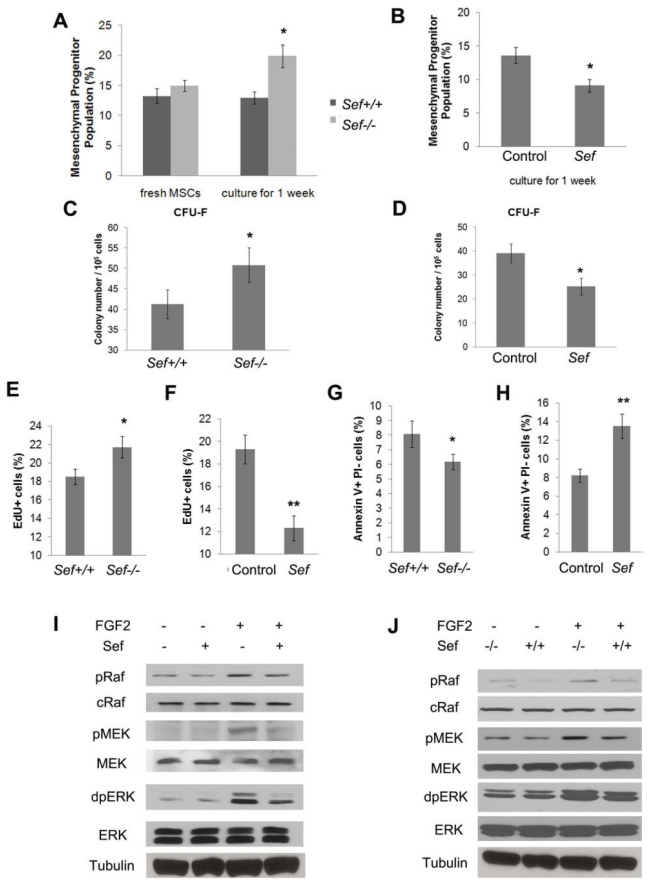

Figure 5. Sef inhibits osteoblast progenitor cell expansion by decreasing progenitor cell proliferation and inducing apoptosis through the FGF/MAPK signaling

(A) Bone marrow cells from *Sef*+/+ and −/− mice were analyzed by flow cytometry for Sca1+CD29+CD45− mesenchymal progenitor cell population, either using freshly isolated bone marrow or adherent bone marrow cells cultured for 1-week. (B) Bone marrow cells from *Sef;Cre-ERT*^{2} double-transgenic and control mice were cultured for 1-week and analyzed by flow cytometry for Sca1+CD29+CD45− mesenchymal progenitor cell population. (C) Bone marrow cells from *Sef*+/+ and *Sef*−/− and (D) bone marrow cells from *Sef;Cre-ERT*^{2} double-transgenic and control mice were cultured for colony-forming efficiency (CFU-F) assay. (E) Bone marrow cells from *Sef*+/+ and *Sef*−/− and, (F) bone marrow cells from *Sef;Cre-ERT*^{2} double-transgenic and control mice were cultured in osteogenic medium and labeled with EdU for 24 hours and analyzed by FACS. (G) Bone marrow cells from *Sef* +/+ and *Sef*−/− and (H) bone marrow cells from *Sef;Cre-ERT*^{2} double-transgenic and control mice were cultured in osteogenic medium, double-labeled with annexin V and propidium iodide followed by flow cytometry to quantify apoptotic cells. (I) Bone marrow cells from *Sef;Cre-ERT*^{2} littermates and (J) bone marrow cells from *Sef*+/+, *Sef*+/−, and *Sef*−/− were starved and stimulated with FGF2 for 10 min and tested for pRaf, pMEK and dpERK activity and cRaf, MEK and ERK1/2 expression levels. (*p<0.05; **p<0.01).

NIH-PA Author Manuscript
NIH-PA Author Manuscript
NIH-PA Author Manuscript

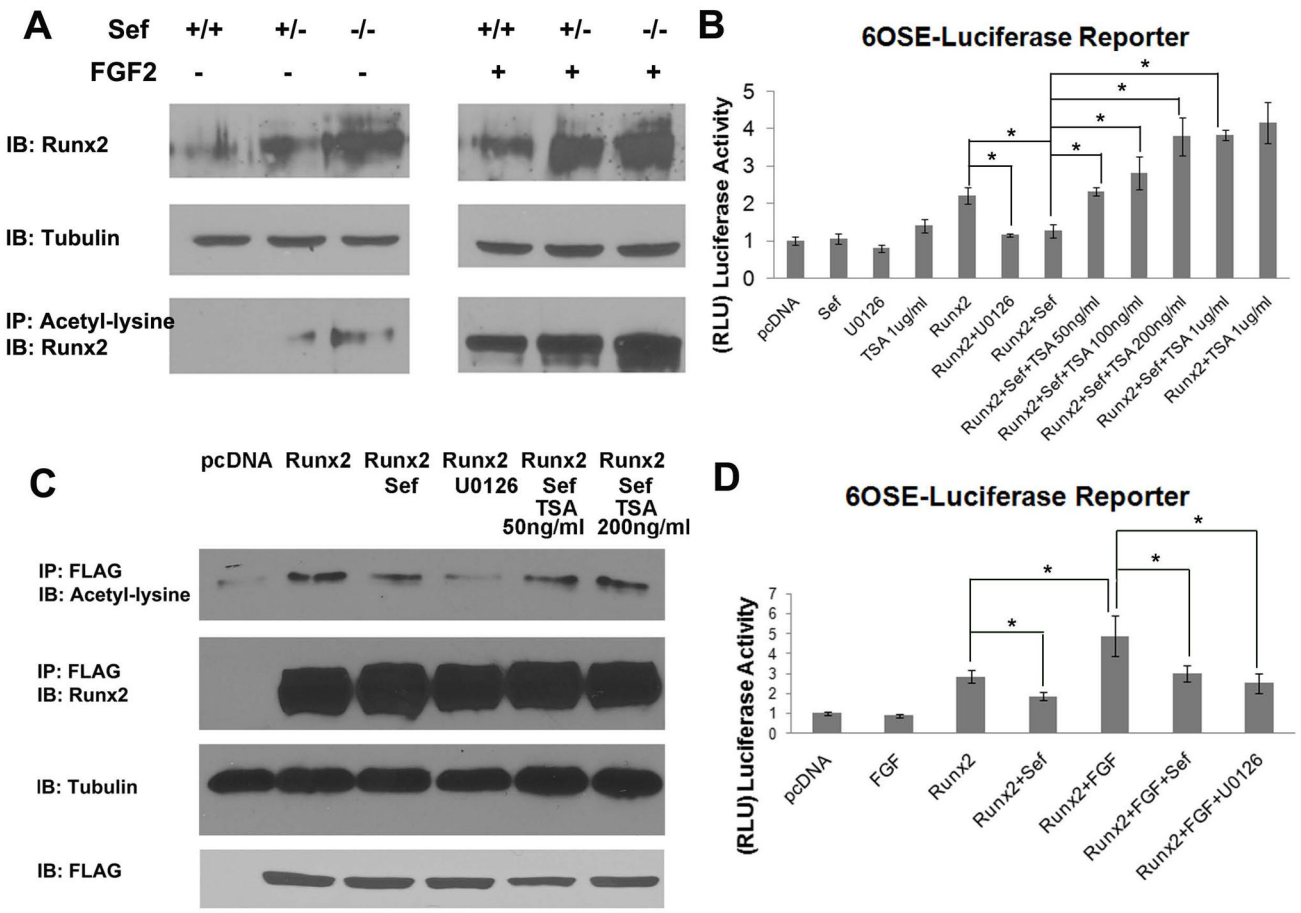

Figure 6. Sef represses FGF/MAPK mediated Runx2 acetylation and transcriptional activation

(A) Bone marrow cells from *Sef*+/+, *Sef*+/−, and *Sef*−/− were stimulated with or without FGF2 after serum starvation and analyzed by immunoblotting for total Runx2 protein levels as well as acetylated Runx2. (B) The 293T cells were co-transfected with 6OSE-luciferase reporter plasmid with Runx2-FLAG, with or without Sef plasmids. 24 hours after transfection, the cells were treated with U0126 or TSA at different concentrations for an additional 24 hrs then assayed for Runx2-induced luciferase reporter activity. (C) The 293T cells were transfected with Runx2-FLAG plasmid with or without Sef expression vectors, and then treated with U0126 or TSA at 50ng/ml or 200ng/ml. cell lysates were subjected to immunoblotting for acetylated Runx2-FLAG and total Runx2-FLAG. Tubulin served as a loading control. (D) The 293T cells were co-transfected with 6OSE-Luciferase reporter gene, Runx2-FLAG, and Sef. The transfected cells were serum starved followed by stimulation with FGF2 for 8 hours and then treated with U0126 overnight to inhibit FGF2 stimulation.

NIH-PA Author Manuscript
NIH-PA Author Manuscript
NIH-PA Author Manuscript

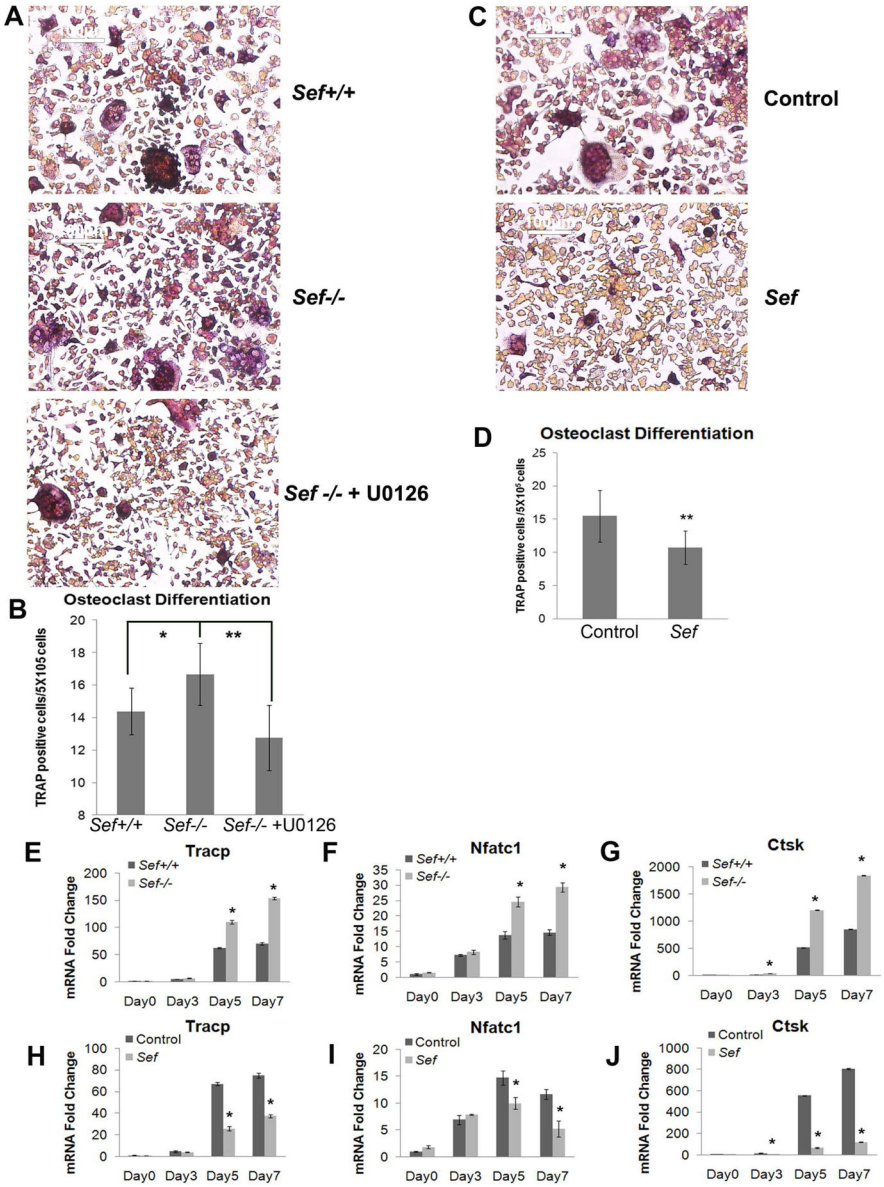

Fig. 7. Sef inhibits osteoclastogenesis in vitro

(A) Bone marrow cells from *Sef*+/+ and *Sef*−/− were induced to differentiate toward the osteoclast lineage with M-SCF and RANKL for 7 days in the presence of absence of the ERK inhibitor U0126 and stained for TRACP and photographed under light microscopy. (B) Quantification of TRACP-stained osteoclasts with more than three nuclei from *Sef*+/+, *Sef*−/− and *Sef*−/− cultured with U0126 in panel A. (C) *Sef;Cre-ERT*^{2} double-transgenic and control littermates were cultured in the presence of M-CSF and RANKL for 7 days and stained for TRACP and photographed under light microscopy. (D) Quantification of TRACP-stained osteoclasts with more than three nuclei for control and *Sef* overexpression cells. (E–G) RT-qPCR analysis showing mRNA expression of osteoclast markers using bone marrow cells isolated from *Sef*+/+ mice and *Sef*−/− as wells as *Sef;Cre-ERT*^{2} double-transgenic and control mice (H–J): (E, H) Tartrate-resistant acid phosphatase; (F, I) Nfact1 and (G, J) Cathepsin K (n=3).

NIH-PA Author Manuscript

NIH-PA Author Manuscript

NIH-PA Author Manuscript

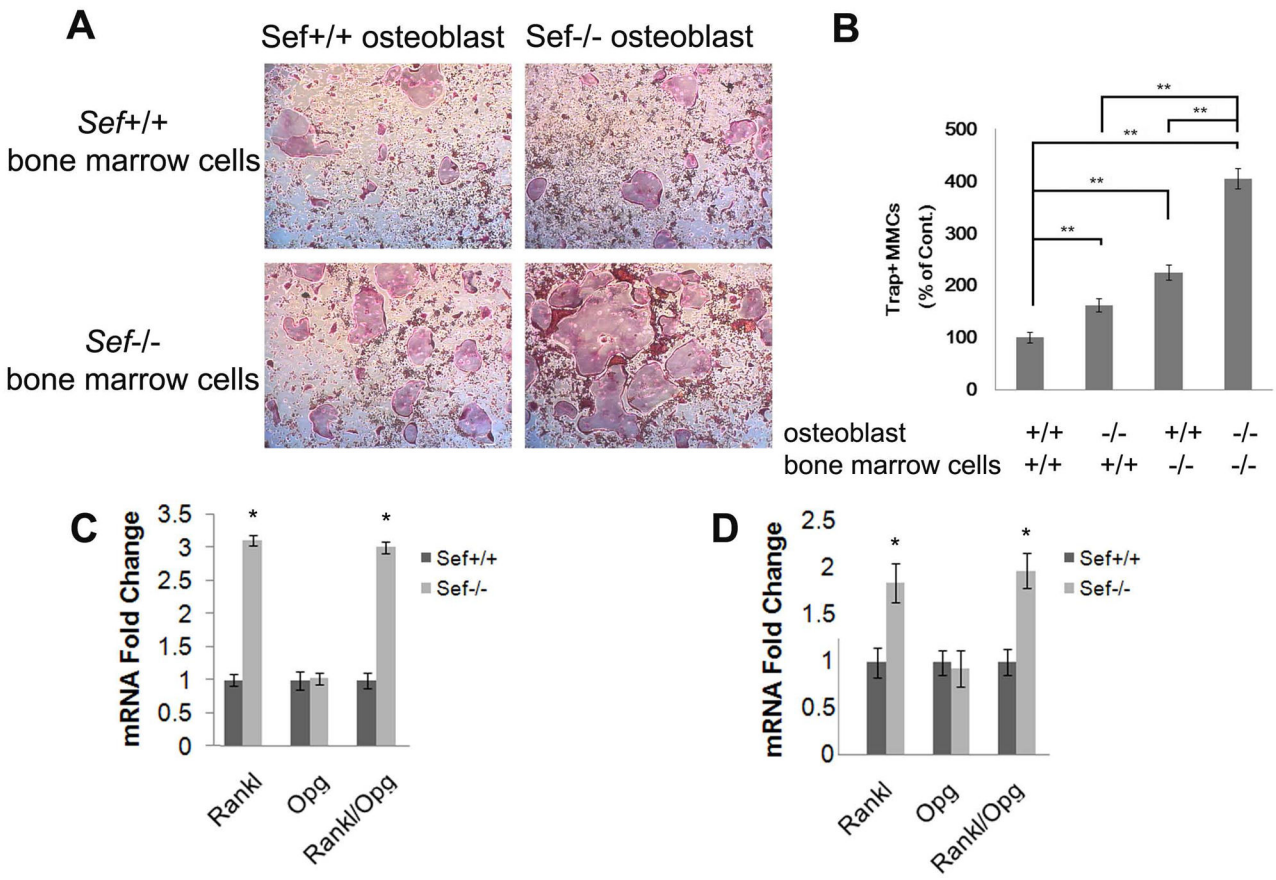

Fig. 8. Sef affects osteoblast-dependent osteoclastogenesis

(A) Calvarial and bone marrow cells from *Sef*+/+ and *Sef*−/− mice were mixed as indicated in 24-well plates and stained for TRACP. (B) Bar graphs indicate the number of $TRACP^+$ multinucleated cells per well (n=6). (C) RNA was extracted from co-cultured calvarial osteoblasts and bone marrow cells and quantified mRNA expression of RANKL and OPG and RANKL/OPG ratio using qRT-PCR (n=3). (D) RNA isolated from distal femur metaphysis were quantified for RANKL, OPG and RANKL/OPG ratio (n=3).

NIH-PA Author Manuscript

NIH-PA Author Manuscript

NIH-PA Author Manuscript

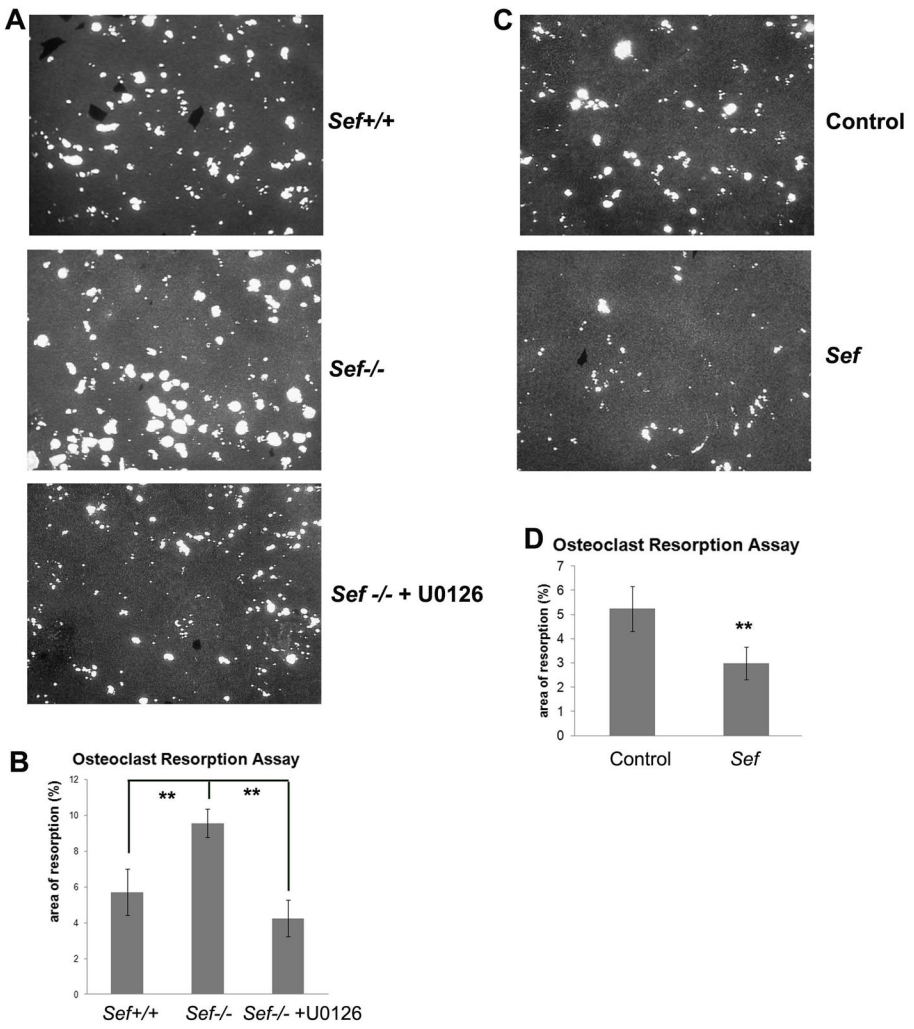

Fig. 9. Sef inhibits osteoclast function

(A) Bone resorption assay using Corning Osteo Assay Surface 96-well plates with bone marrow-derived osteoclasts from *Sef*+/+ or *Sef*−/− mice cultured with or without U0126 for 14 days. (B) Quantification of resorption area of *Sef*+/+, *Sef*−/− and *Sef*−/− with U0126 (n=16). (C) Bone resorption assay of bone marrow derived from *Sef;Cre-ERT*^{2} double-transgenic mice and control littermates. (D) Quantification of resorption area (n=16). ***p*<0.01.

NIH-PA Author Manuscript
NIH-PA Author Manuscript
NIH-PA Author Manuscript

Table 1

Cortical Histomorphometric Parameters of Femoral Metaphysis

	Male	
	***Sef*+/+ (n=6)**	***Sef*−/− (n=6)**
N.Ob/Ec.Pm (mm^{-1})	3.76±1.78	7.56±2.42*
N.Oc/Ec.Pm (mm^{-1})	0.45±0.38	0.27±0.28
N.Ot/Ct.B.Ar	2325.45±440.32	2331.69±429.76
Ct.B.Ar	0.56±0.13	0.54±0.08
Ct.BV/TV (%)	30.12±3.89	30.46±5.04
Ct.Th (μm)	194.95±39.20	188.35±30.82
Ps.Pm (mm)	5.72±0.27	5.71±0.16
Ps.dL.S/BS	59.20±16.50	47.51±8.22
Ps.MAR (μm/day)	1.70±0.25	1.55±0.26
Ps.BFR/BS	1.03±0.43	0.75±0.24
Ec.Pm (mm)	4.49±0.17	4.92±0.83
Ec.dL.S/BS	44.52±22.06	31.97±14.63
Ec.MAR (μm/day)	1.38±0.40	1.40±0.22
Ec.BFR/BS	0.68±0.44	0.46±0.24
Ec.OS/BS (%)	90.7912±13.13	83.2633±9.85
Ec.ES/BS (%)	1.14±0.99	0.95±0.95
Ec.Oc.S/BS (%)	0.57±0.42	0.38±0.41

N.Ob = number of osteoblasts; N.Oc = number of osteoclasts; N.Ot = number of osteocytes; Ec = endocortical; Pm = perimeter; Ct.B.Ar = cortical bone area; Ct.BV/TV = cortical bone volume/tissue volume; Ct.Th = cortical thickness; Ps.Pm = periosteal perimeter; Ps.dL.S/BS = periosteal surface/bone surface; Ec.Pm = endocortical perimeter; OS = osteoid surface; ES = eroded surface.

NIH-PA Author Manuscript
NIH-PA Author Manuscript
NIH-PA Author Manuscript

Table 2

Trabecular Histomorphometric Parameters of Femoral Metaphysis

	Male		Female	
	***Sef*+/+ (n=6)**	***Sef*−/− (n=8)**	***Sef*+/+ (n=6)**	***Sef*−/− (n=5)**
BV/TV (%)	21.55±5.42	19.74±3.28	7.02±0.56	5.75±1.31
OS/BS (%)	0.83±0.54	0.93±0.64	2.38±1.71	3.53±1.86
ES/BS (%)	15.18±3.41	15.96±4.16	18.78±2.60	23.08±3.76
ObS/BS (%)	10.87±3.06	12.60±2.81	18.50±5.29	22.16±3.35
OcS/BS (%)	8.42±1.62	9.01±1.95	11.29±1.50	13.99±2.08*
TbTh (μm)	45.07±9.08	43.45±5.32	28.53±1.07	27.32±3.56
NOb/Tar (mm^{-2})	111.75±29.79	121.48±30.51	94.33±18.21	96.53±11.71
NOb/BPm (mm^{-1})	12.05±4.23	13.46±3.44	19.50±5.18	23.43±4.07
NOc/Tar (mm^{-2})	47.45±11.58	49.96±13.35	34.34±6.36	36.50±7.52
NOc/BPm (mm^{-1})	5.01±1.07	5.46±1.20	6.94±0.82	8.74±1.43*
TbN (mm^{-1})	4.73±0.52	4.55±0.52	2.46±0.23	2.08±0.22*
TbSp (μm)	168.65±32.73	178.91±26.37	380.42±38.63	457.16±54.58*
MS/BS (%)	9.83±1.80	8.79±2.76	5.12±1.62	6.19±4.18
MAR (μm/day)	1.55±0.04	1.46±0.17	1.80±0.33	1.93±0.26
BFR/BS	0.15±0.03	0.13±0.04	0.09±0.04	0.12±0.07

BV = bone volume; TV = tissue volume; OS = osteoid surface; ES = eroded surface; Ob = osteoblast; Oc = osteoclast; BS = bone surface; TbTh = trabecular thickness; Nob = number of osteoblasts; NOc= number of osteoclasts; Tar = tissue area; BPm = bone perimeter; TbN = trabecular number; TbSp = trabecular separation; MS = mineralizing surface; MAR = mineral apposition rate; BFR = bone formation rate.

* $p<0.05$ versus *Sef*+/+ wild type controls.